

## Supporting Information

### **The Critical Role of Water Content in the Electrolyte on the Reversible Electrochemical Performance of Zn-VPO<sub>4</sub>F Cell**

Hooman Yaghoobnejad Asl,<sup>a</sup> Shyam Sharma<sup>a</sup> and Arumugam  
Manthiram<sup>\*a</sup>

<sup>a</sup> *Materials Science and Engineering Program and Texas Materials Institute, The University of Texas at Austin, Austin, Texas 78712, United States. \* Email: rmanth@mail.utexas.edu*

## Synthesis of the VPO<sub>4</sub>F/C active material

The initial LiVPO<sub>4</sub>F/C composite cathode was synthesized according to the Barker method,<sup>1</sup> with some modifications. First, V<sub>2</sub>O<sub>5</sub> was reduced to V(III) with excess oxalic acid and then reacted with stoichiometric NH<sub>4</sub>H<sub>2</sub>PO<sub>4</sub> in water to form an amorphous VPO<sub>4</sub> precursor. The solvent was evaporated, and the solid residue was mixed and ball-milled with super-P carbon (wt. C : wt. VPO<sub>4</sub> = 0.25:0.75). The mixture was then heated at 800 °C for 8 h to form the crystalline VPO<sub>4</sub>/C composite. Next, slightly excess LiF and the VPO<sub>4</sub>/C composite were ball-milled and pressed into pellets, which were heated under vacuum at 650 °C for 0.5 h to form a mixture of LiVPO<sub>4</sub>F/C and residual LiF (Figure S1). Finally, 1.5 g of the obtained lithiated vanadium phosphate fluoride was treated with 25% excess NO<sub>2</sub>BF<sub>4</sub> in ~ 35 mL of anhydrous acetonitrile under N<sub>2</sub> flow and stirred continuously for the delithiation to occur. The delithiation process needed to be repeated once more to get ~ 96% pure VPO<sub>4</sub>F/C and some 4 % (by weight) of LiVPO<sub>4</sub>F/C, as indicated by the quantitative phase analysis of the X-ray diffraction pattern (Figure 1).

## Materials characterization

Powder X-ray diffraction (XRD) patterns of various samples were recorded with a Rigaku Miniflex 600 diffractometer, operating with a Cu K<sub>α</sub> source, and the data were refined with GSAS-II software.<sup>2</sup> A Kratos X-ray photoelectron spectrometer was used to collect the XPS spectra of the charged and discharged electrodes, with a monochromatized Al K<sub>α</sub> radiation as the excitation source, and Casa XPS software was used for fitting the observed features. The morphology and elemental analyses of the samples were carried out with a Vega TESCAN thermionic source scanning electron microscope (SEM) equipped with a Bruker XFlash energy dispersive X-ray spectrometer (EDXS). Furthermore, the composition of the discharged electrode was quantified with inductively coupled plasma – optical emission spectroscopy (ICP-OES) via a Varian 715-ES spectrometer. Also, the amount of residual carbon/volatile species present in the VPO<sub>4</sub>F/C composite electrode was assessed through simultaneous thermal analysis (STA) with a Netzsch STA 449 Jupiter system. These results (Figure S2) were used for calculations of the observed capacity from the electrochemical tests. Finally, the redox titration was carried out in an automated titrator in the iodometric mode, with a potentiometric equivalence-point detection. Quantification of the water content of the ZnCl<sub>2</sub> – urea electrolyte was carried out via FTIR-ATR spectroscopy with a Thermo Scientific Nicolet iS5 FT-IR spectrometer equipped with iD7 ATR accessory. Details of the analyses are provided in Figure S5.

## Electrochemical testing

Due to the corrosive nature of the electrolytes used in this work and the relatively high oxidizing potentials applied, the standard stainless steel coin-cell architecture could not be used for electrochemical studies. Instead, a special flooded borosilicate glass cell was designed (shown schematically in Figure S3). This cell configuration avoided any contact between the electrolyte and the metallic current collectors, thereby allowing for scanning the potential to the anodic limit of the electrolyte without any interference from current collector corrosion. The cells were operated while submerged in a thermostatted oil bath to decrease the viscosity of the ionic liquid electrolyte. The VPO<sub>4</sub>F/C electrodes were prepared

---

<sup>1</sup> J. Barker, M. Y. Saidi and J. L. Swoyer, *J. Electrochem. Soc.*, 2003, **150**, A1394.

<sup>2</sup> B. H. Toby and R. B. Von Dreele, *J. Appl. Crystallogr.*, 2013, **46**, 544–549.

through ball-milling the delithiated powder with conductive carbon for 1 h, followed by an addition of PVDF/NMP, so that the overall weight fraction of the electrode was  $\text{VPO}_4\text{F/C} : \text{Super-P} : \text{PVDF} = 0.70 : 0.15 : 0.15$ . The slurry was then drop-casted onto boron-doped silicon wafers (electronic conductivity =  $100 \text{ S.cm}^{-1}$ ), which served as current collectors, and dried in a vacuum oven overnight at  $120 \text{ }^\circ\text{C}$ . The dried electrode-Si composite was then attached to a graphite rod with conductive carbon glue and transferred into an Ar glove box for cell assembly. The glass cell was assembled with Zn as the negative electrode and  $\text{ZnCl}_2\text{-(NH}_2)_2\text{CO}$  ionic liquid as the electrolyte and sealed. The cells loaded with the aqueous electrolyte were assembled under ambient conditions. Galvanostatic charge-discharge measurements, along with galvanostatic intermittent titration (GITT) tests, were carried out with a Biologic VMP3 multichannel potentiostat.

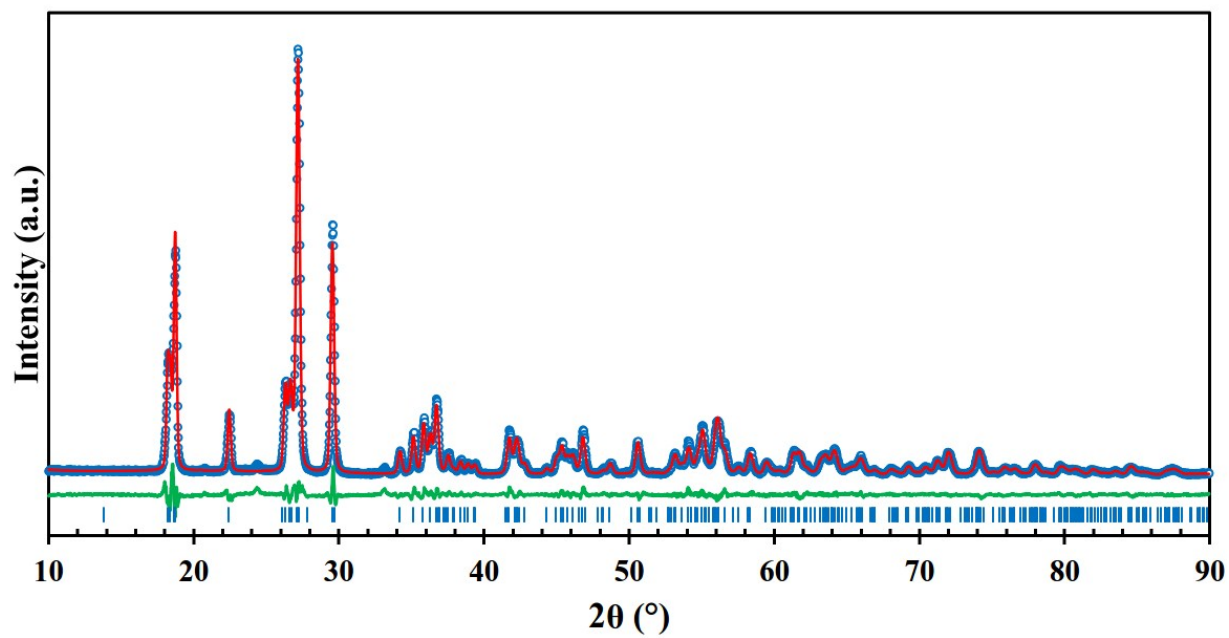


Figure S1. Rietveld refinement of the as-synthesized  $\text{LiVPO}_4\text{F}$  electrode. The phase is practically pure with less than 1% wt. of unreacted  $\text{VPO}_4$  impurity.

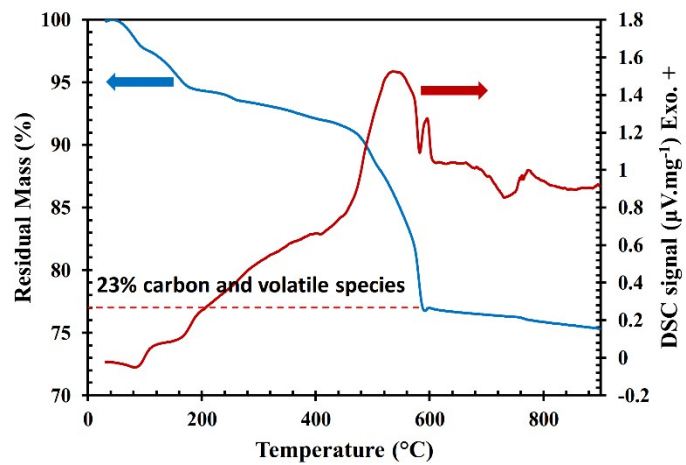


Figure S2. TGA-DSC curves of the delithiated VPO<sub>4</sub>F/C composite carried out in air with a heating rate of 10 °C min<sup>-1</sup>.

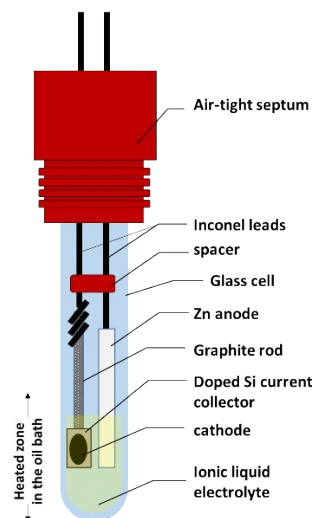


Figure S3. Schematic representation of the flooded electrochemical cell designed for testing the Zn-VPO<sub>4</sub>F system.

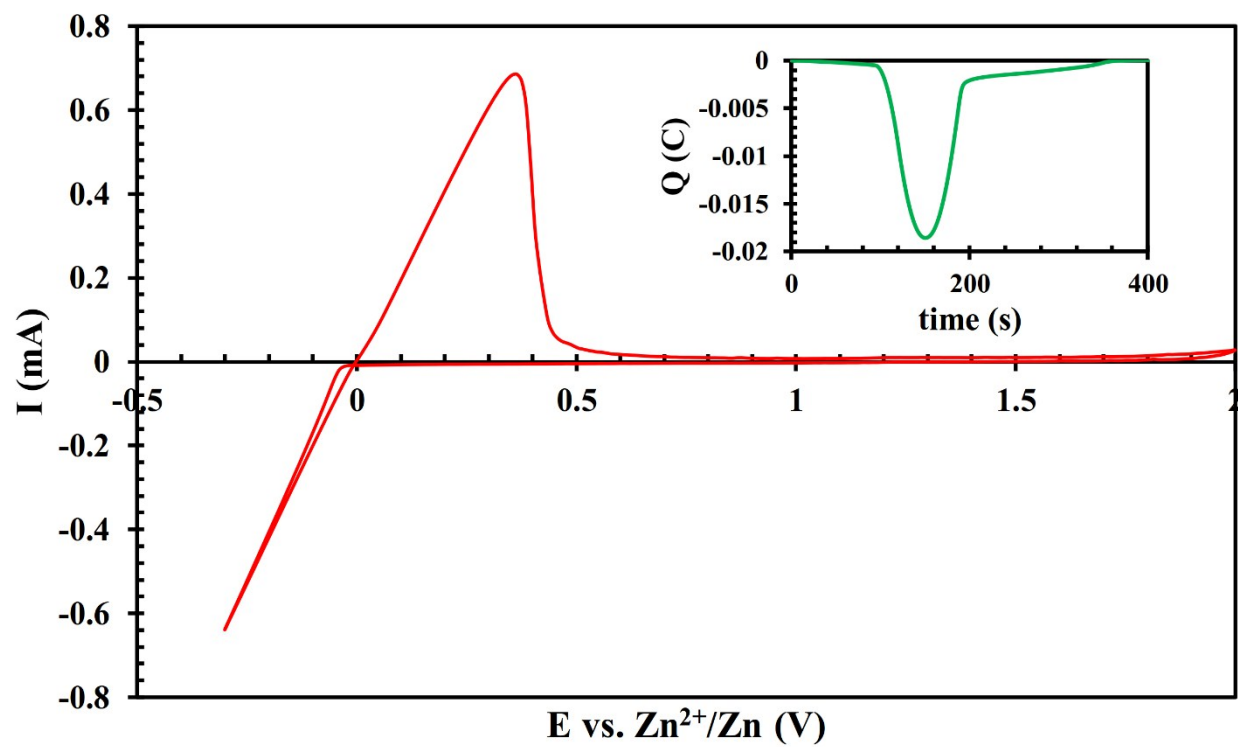


Figure S4. Cyclic voltammetry curve for the Zn electrodeposition-stripping in the blank system. The inset shows the zinc coulombic efficiency during one cycle.

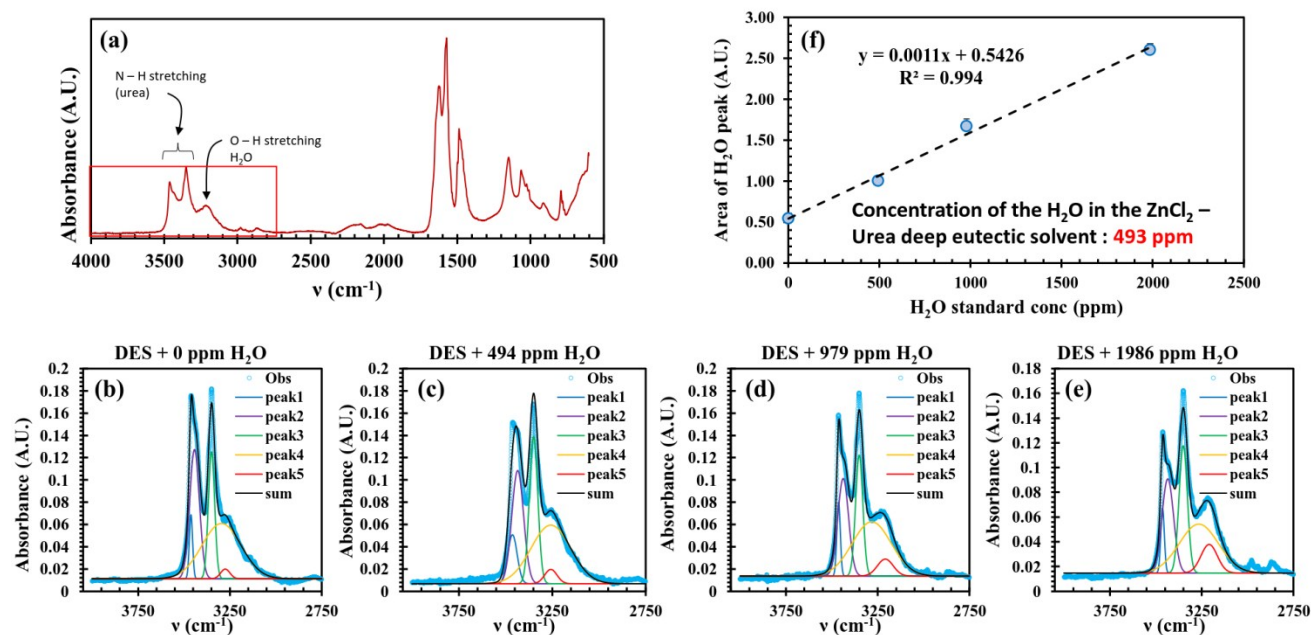


Figure S5. FTIR-ATR determination of the moisture concentration in the  $\text{ZnCl}_2$  – urea DES electrolyte by the standard addition method. (a) The FT-IR spectrum of the as-prepared DES electrolyte with 1986 ppm  $\text{H}_2\text{O}$  added; the peak positions for various stretching frequencies are marked. (b-e) Peak deconvolution and quantification for calibration curve construction. The peaks 1 - 4 belong to various vibrations due to the di-amide group while peak 5 is due to the O-H stretching in water. (f) Calibration curve obtained from (b-e) and following the standards addition method.



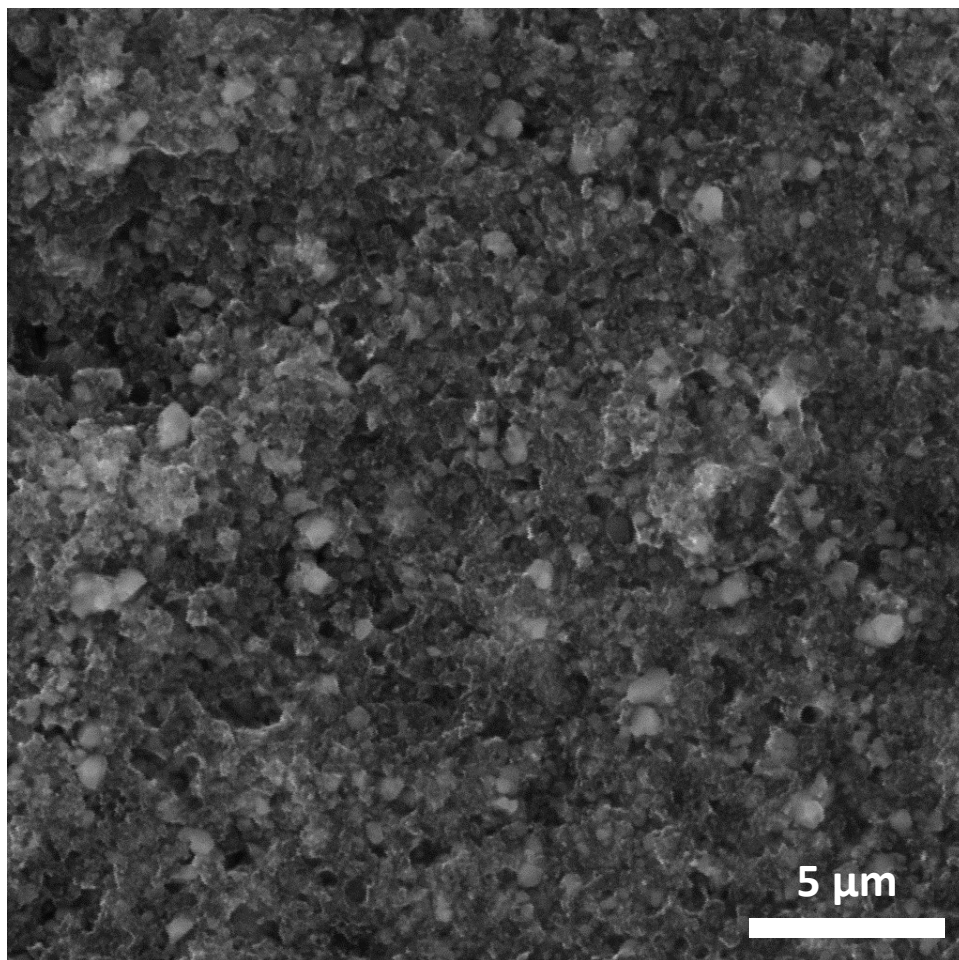


Figure S6. The backscattered electron image of the VPO<sub>4</sub>F/C electrode with the PVDF binder. The brighter VPO<sub>4</sub>F/C particles can be discriminated from the darker carbon-based matrix due to the Z-contrast effect. The average particle size of the VPO<sub>4</sub>F/C is approximately 1 μm.

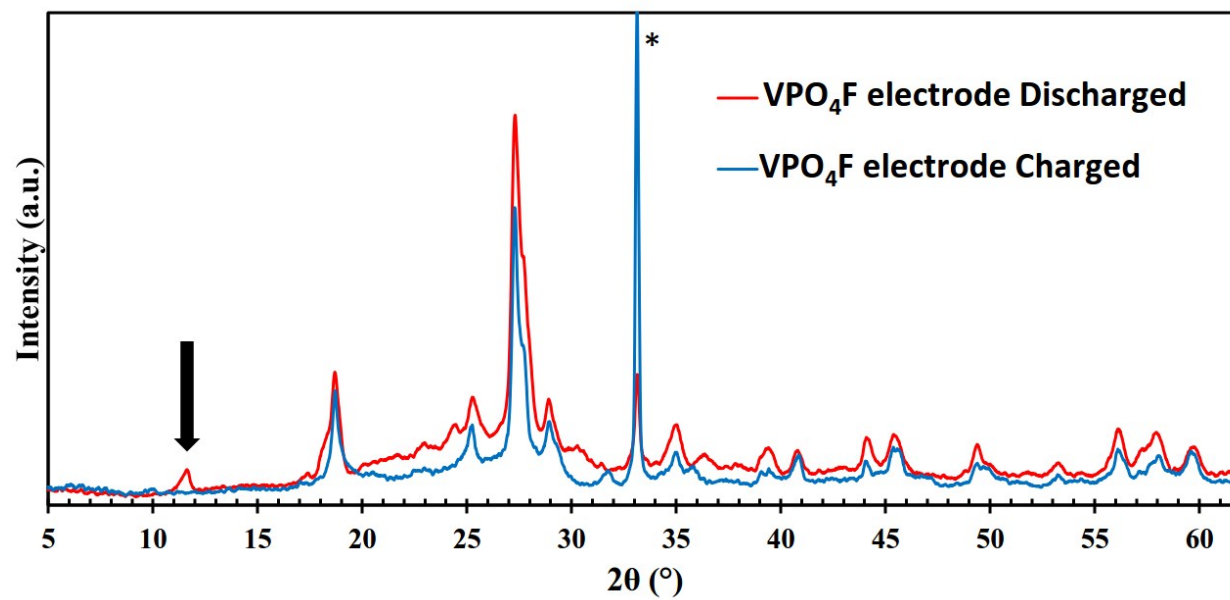


Figure S7. Ex-situ XRD patterns of the electrochemically cycled VPO<sub>4</sub>F electrode in the Zn-VPO<sub>4</sub>F system. The impurity peak at  $2\theta = 33.2^\circ$  indicated with the asterisk is probably due to the electrolyte salt residual on the surface of the electrode. The broad low-angle peak around  $11.5^\circ$  is marked with an arrow.

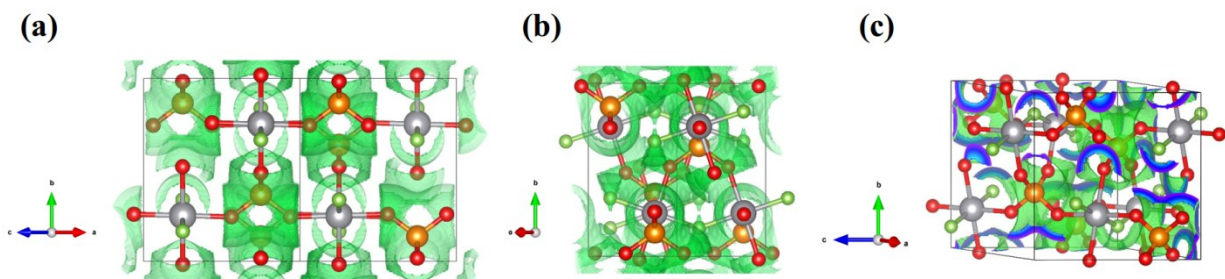


Figure S8. The calculated Bond Valence Sum (BVS) map for H<sup>+</sup> in VPO<sub>4</sub>F host as viewed along the (a) [101], (b) [10-1], and (c) a general direction. For all images,  $\Delta V = 0.3$  valence units.

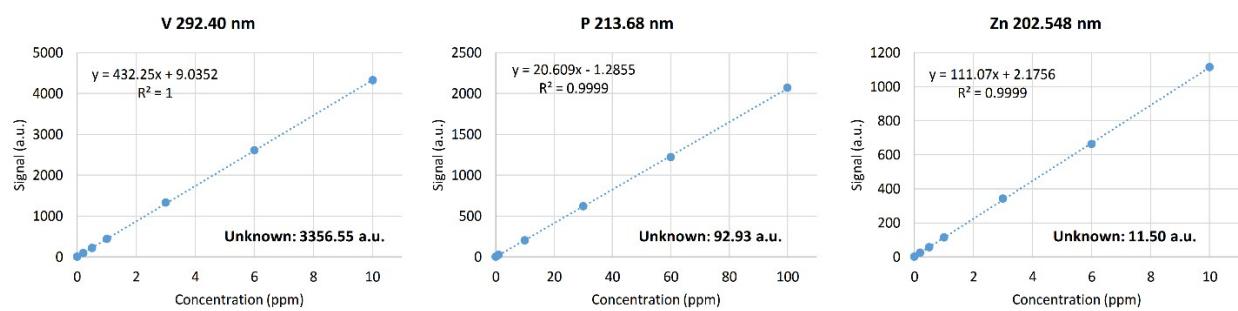


Figure S9. Quantification curves for the discharged electrode composition analysis via ICP-OES.